Optical Materials 148 (2024) 114941

Contents lists available at ScienceDirect

Optical Materials

journal homepage: www.elsevier.com/locate/optmat

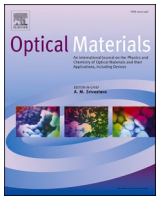

Research Article

Synthesis and characterizations of Ce-doped ZnO thin films for radiation shielding

Ali Kemal Soğuksu [a,*], Süleyman Kerli [b], Yusuf Kavun [c,d], Ümit Alver [e]

[a] Department of Material Science and Engineering, Kahramanmaraş Istiklal University, Kahramanmaraş, Turkey
[b] Department of Energy Systems Engineering, Kahramanmaraş Istiklal University, Kahramanmaraş, Turkey
[c] Department of Material Science and Engineering, Graduate School of Natural and Applied Sciences, Kahramanmaraş Sütçü İmam University, Kahramanmaraş, Turkey
[d] Vocational School of Health Services, Dept. of Medical Imaging Techniques, Kahramanmaras Sütçü Imam University, Kahramanmaras, Turkey
[e] Metallurgical and Materials Engineering, Karadeniz Technical University, Trabzon, Turkey

ARTICLE INFO

Keywords:
Thin film
Gamma
NaI(Tl) detector

ABSTRACT

In this research, different amounts of Ce-doped ZnO thin films were synthesized using the spray pyrolysis method. Structural, morphological and optical properties of these synthesized films were investigated. In XRD analyses, wurtzite (hexagonal) structures were observed in the films. In SEM analysis, there were changes in the surface morphology of the films with doping, and in cross-section measurement, the thickness of the films was measured to be approximately 1.2 μm. In UV–vis spectrometry analysis, it is seen that the effect of Cerium contribution on optical transmittance and band gap positively affects shielding. NaI(Tl) detector and gamma energies of 384, 1173, and 1333 keV have been used to investigate the radiation protection properties of these synthesized films. As a result of these measurements, linear attenuation coefficient (LAC) values have been obtained. Radiation shielding parameters have been calculated with these (LAC) values. The Mass Attenuation Coefficient (MAC), Half Value Layer (HVL), Tenth Value Layer TVL (and) Mean Free Path (MFP) values have been also calculated using this LAC result. According to these results, Ce-doped ZnO films were found to be effective in radiation shielding.

1. Introduction

The world is witnessing an increasing interest in the use of radioactive sources as an alternative within applications in energy production, the health sector, and military fields [1–3]. This interest leads to involuntary exposure to radiation and poses a threat to health. For this reason, materials developed for radiation protection have become very important and many researchers have been working on developing radiation protection materials for a long time [4–6].

Among these developed materials, it is known that some materials such as lead with a high atomic number are used to prevent exposure to radiation [7]. However, in addition to the many advantages of such materials, they also have disadvantages such as non-transparency (opacity) and toxic effects on the environment [8].

In recent years, products that can be used as radiation shielding materials (easy to manufacture, cheap [8] and light-weight, non-toxic, non-opaque) have attracted attention specifically, glass materials are at the forefront of these products. Glass materials and thin films coated on glass materials with different methods have been the subject of many researches [9–15].

Thin film is a layer of material whose thickness varies from 1 nm to several micrometers. Thin films have a critical function in the development and study of new materials with unique properties [16–19]. Thin films are produced by production methods such as thermal evaporation [20], sol-gel [21], RF [22], chemical vapor deposition [23], spray pyrolysis [24]. The spray pyrolysis method is easy to apply and cost-effective among these methods [25].

In addition, thin film types depending on the type of materials used; Inorganic/Organic thin films [26], Semiconductor thin films [27], Transparent conductive thin films [28], Superconducting thin films [29], Pyroelectric films [30], and Ferroelectric thin films [31].

Semiconductor metal oxide thin films attract researchers due to their outstanding thermal and chemical stability [32]. Furthermore, an in-depth investigation of the physical properties of semiconductor metal oxide thin film structures is significant for the design of new and high-precision radiation dosimeters [33].

* Corresponding author.
E-mail address: kemalsoguksu@gmail.com (A.K. Soğuksu).

https://doi.org/10.1016/j.optmat.2024.114941
Received 21 November 2023; Received in revised form 16 January 2024; Accepted 17 January 2024
Available online 24 January 2024

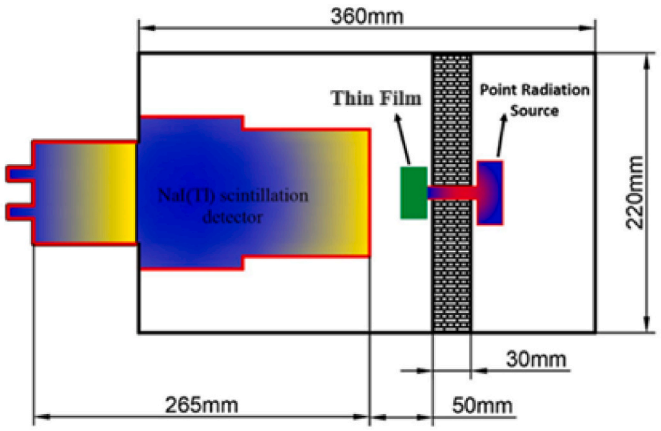

Fig. 1. Radiation experimental setup for Ce-doped ZnO thin films [41].

Zinc oxide (ZnO) is indeed a semiconductor material with a high/direct band gap, and it exhibits a significant exciton binding energy. The specific values for the band gap and exciton binding energy for ZnO are approximately 3.37 eV (eV) for the band gap and around 60 meV (meV) for the exciton binding energy [34,35]. These properties make ZnO a versatile and interesting material for various applications. In addition, recent studies on zinc oxide have been reported to improve radiation shielding performance [36]. The additive is available in the literature where it is an effective way to improve and enhance the properties of ZnO thin films [34]. Zinc oxide films were synthesized by making various doping and different properties were investigated [5,37–39].

In this study, the effects of undoped and Cerium-doped ZnO thin films on optical, structural and shielding properties were investigated. The thin films produced were produced through the spray pyrolysis method. According to the results obtained, it was observed that the linear attenuation coefficient values required for the radiation shielding increased due to the Cerium-doped ZnO films. These results show that Cerium-doped ZnO films can be used as a radiation shielding material.

2. Experimental

Undoped and Cerium doped Zinc oxide thin films were deposited on glass substrates at 400 °C at 0.1 M ratio using spray pyrolysis technique. The solutions (50 ml) of pure and Ce-doped ZnO were prepared for depositing thin films by using zinc nitrate hexahydrate ($Zn(NO_3)_2 \bullet 6H_2O$) as a precursor, and cerium (III) nitrate hexahydrate ($Ce(NO_3)_3 \bullet 6H_2O$) as a dopant, respectively. To eliminate the surface impurities, the slides were cleaned ultrasonically in ethyl alcohol for 10 min. Cerium (III) nitrate hexahydrate ($Ce(NO_3)_3 \bullet 6H_2O$) molar doping ratios are 0 %, 2.5 %, 5 % and 10 %, respectively. The prepared solution was sprayed on glass substrates heated at 400 °C using airbrush spray. Thin films obtained after sputtering were annealed at 550 °C for 2 h.

The crystal structures of the prepared undoped and Ce-doped ZnO films were investigated with the Philips X'Pert Pro X-ray diffractometer (XRD) with Cu-Kα radiation. The surface morphology of the films was observed using field scanning electron microscopy (SEM). The optical properties of the films were examined with the UV–vis(Shimadzu UV-1800) spectrometer.

2.1. Radiation measurements

In this study, the effects of some Cerium-doped ZnO thin films on the optical, structural and shielding effectiveness have been examined. In the experimental setup of radiation shielding properties shown in Fig. 1, ^{133}Ba 384 keV, ^{60}Co 1173 keV and ^{60}Co 1333 keV energized gamma ray were used. Additionally, experiments were performed with a NaI(Tl) (ORTEC® 905-4) detector [40].

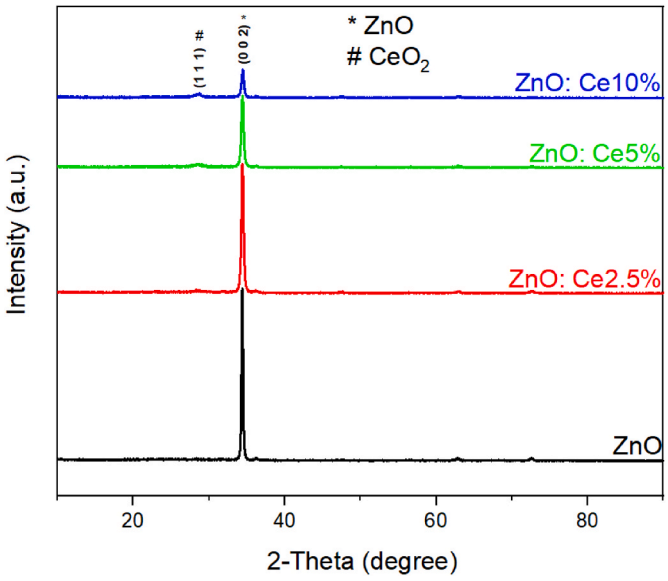

Fig. 2. X-ray diffraction pattern of undoped and Ce-doped ZnO thin films.

The spray pyrolysis method was used to produce thin films and the Lambert-Beer law was used to reveal the radiation shielding properties of the films [42]. In the Lambert-Beer law given in Eq. (1), x is the thickness of the thin film, I_0 is the amount of gamma ray measured by the detector without placing thin films in the experimental system, and I is the amount of gamma ray measured after placing thin films in the experimental setup. μ is the linear attenuation coefficient (LAC) [40].

$$\mu = \ln\left(\frac{I}{I_0}\right) \Big/ (-x) \ (\mathrm{cm}^{-1}) \tag{1}$$

The standard deviations of the measurements of these thin films are calculated by Eq. (2) here $\overline{\mu}$ is the average LAC number, μ_i of each measurement and N is the measurement number [42].

$$\sigma = \sqrt{\frac{\sum_{i=1}^{N}(\mu_i - \overline{\mu})^2}{N-1}} \tag{2}$$

The film thickness required to transmit half of the gammas interacting with thin films is given by Half Value Layer (HVL), and the film thickness required to transmit one tenth is given by Tenth value layer (TVL). In addition, the path that gammas can take within the film is given by Mean Free Path (MFP) and these are given in equations (3)–(5) [42].

$$Half\ Value\ Layer\ (HVL) = \frac{\ln 2}{\mu}\ (\mathrm{cm}) \tag{3}$$

$$Tenth\ Value\ Layer\ (TVL) = \frac{\ln 10}{\mu}(\mathrm{cm}) \tag{4}$$

$$Mean\ Free\ Path\ (MFP) = \frac{1}{\mu}(\mathrm{cm}) \tag{5}$$

3. Results

Fig. 2 shows the X-ray diffraction spectrum of undoped and Ce-doped ZnO thin films annealed at 550 °C. The ZnO (002) peak has a wurtzite (hexagonal) structure at 34.45°. The CeO_2 (111) peak is cubic at 28.58°. In addition, no peaks due to impurities were detected. The diffraction peaks corresponding to ZnO and CeO_2 were found to be consistent with standard Reference code:00-036-1451 and Reference code:00-043-1002, respectively. The examination of thin film samples showed that Ce-doped ZnO film was formed due to the increase in Ce doping ratio. It

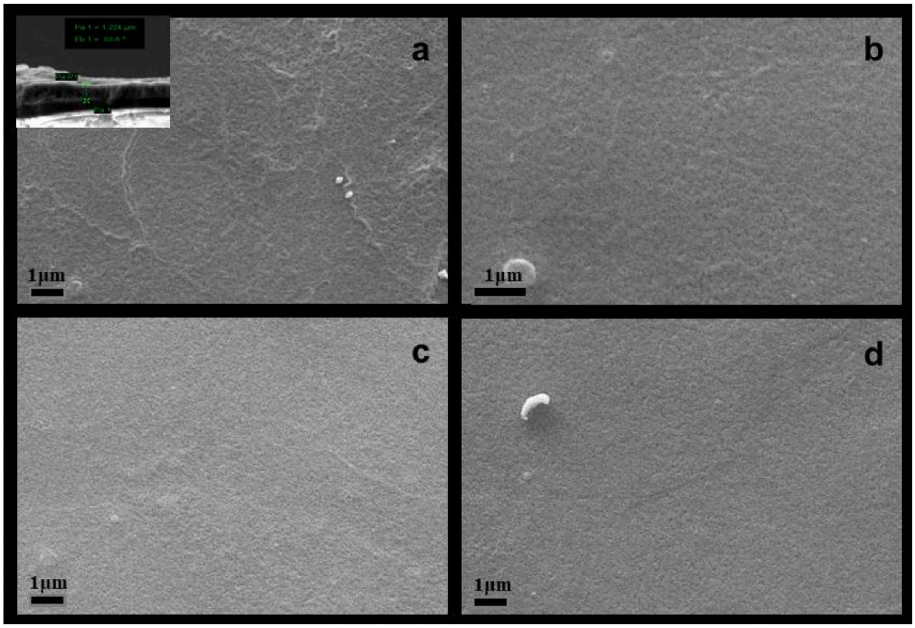

Fig. 3. SEM images of a) undoped ZnO, b) ZnO:Ce2.5 %, c) ZnO:Ce5%, d) ZnO:Ce10 % doped thin films. The cross section of undoped ZnO thin films is also shown.

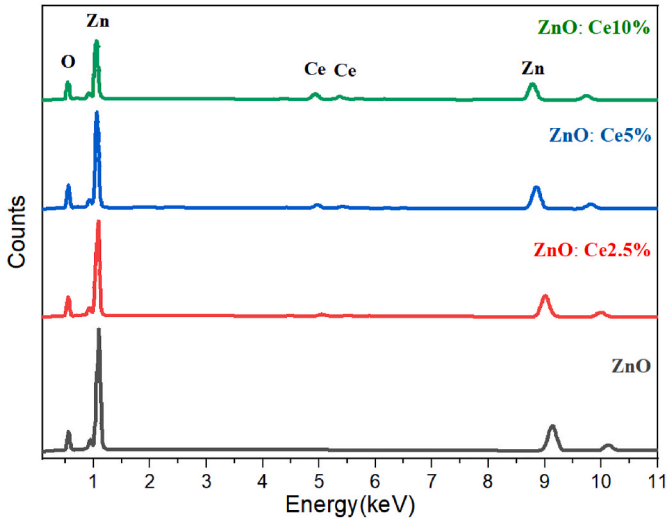

Fig. 4. EDAX spectrum of Ce-doped ZnO thin films.

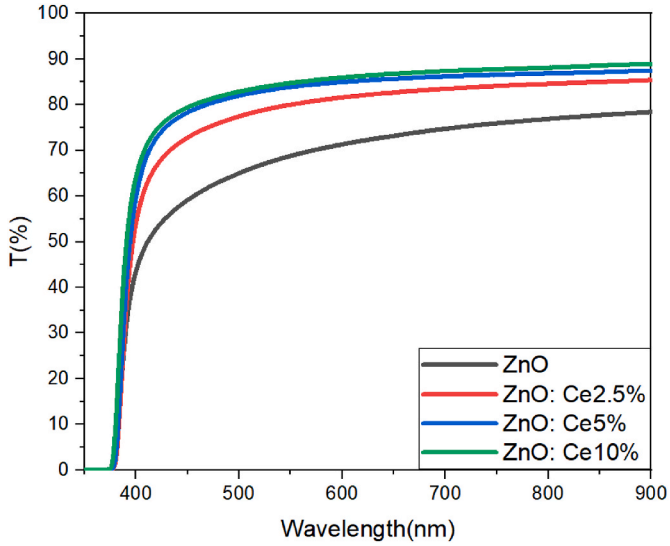

Fig. 5. The optical transmission spectra of undoped and Ce-doped ZnO thin films.

can also be said that the (002) diffraction peak grows along the c-axis orientation of the undoped and Ce-doped ZnO thin films [43].

Fig. 3 shows the SEM micrograph of undoped and Ce-doped ZnO thin films. In SEM images, the average thickness of the synthesized samples was measured as approximately 1.2 μm. It was observed that the increase in the cerium additive ratio in the cerium doped ZnO thin film samples caused changes in the surface morphology. Fig. 4 shows the Energy Dissipative X-ray Spectrometer (EDAX) image that clearly shows the presence of Zn, O, and Ce elements in the Ce-doped ZnO thin film samples. In EDAX spectrum analysis, it is seen that ZnO peaks decrease and CeO_2 peaks increase due to the increase in Ce dope. Energy Dissipative X-ray Spectrometer (EDAX) images match the literature [44,45].

Optical transmission spectra of undoped ZnO and Ce-doped ZnO thin films were measured by UV–visible spectrophotometer in the 350–900 nm range as shown in Fig. 5. Fig. 6 shows the absorbance graph of the samples. Depending on the increase in Ce doping ratio, the optical transmittance increased in the visible region ranges. It was seen that the ZnO:Ce10 % film had the highest optical transmittance and the lowest absorbance value. Optical transmittance values were ZnO (78 %), ZnO: Ce2.5 % (85 %), ZnO:Ce5% (87 %), ZnO:Ce10 % (89 %), respectively. The optical transmittance of nanostructured products mainly depends on impurities and crystallite defects [46].

Doping in ZnO films causes a direct wide-band gap modification of the semiconductor since it causes crystal defect [46]. In Fig. 7, the optical band gap of undoped ZnO and Ce-doped ZnO thin films were determined using the Tauc model [47]. It was observed that Ce doping increased the band gap of ZnO from about 3.24 to 3.27 (eV), studies with similar results are available in the literature [40,48]. Ce-doped ZnO is a natural n-type semiconductor material, and the Fermi level will move above or below the conduction band when increased carriers due to Ce doping fill the conduction band. Consequently, the distance covered by vertical transitions of electrons from the valence band to the conduction band expands [40].

Fig. 8 shows the Linear Attenuation Coefficient (LAC) of Ce-doped

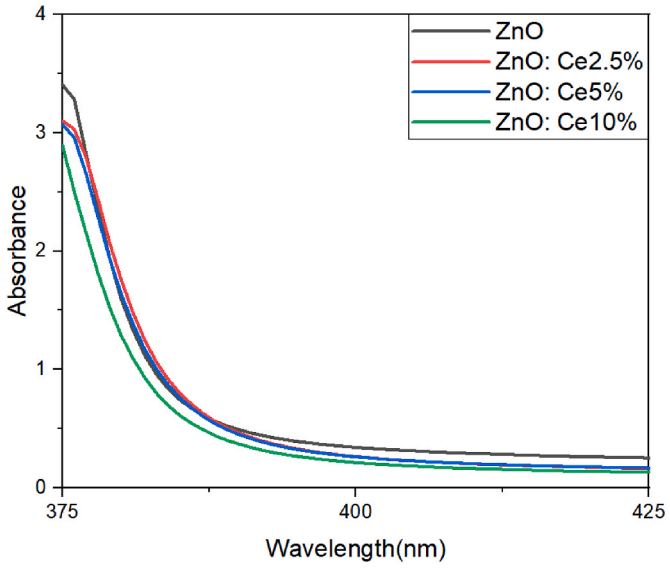

Fig. 6. UV–vis absorbance of undoped and Ce-doped ZnO thin films.

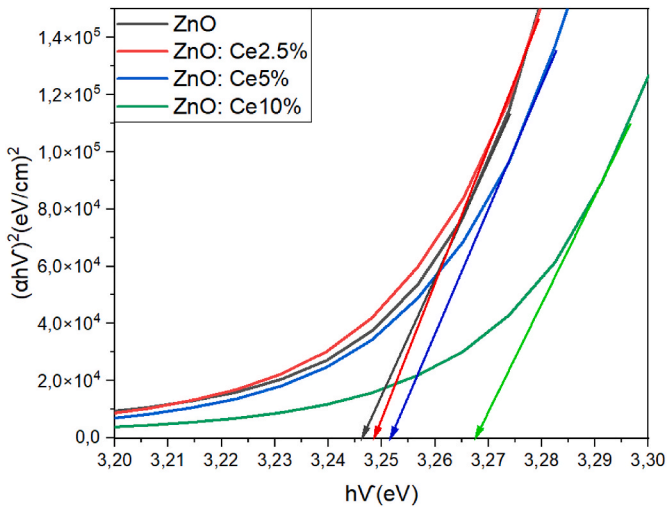

Fig. 7. Tauc's plots for band gap of the undoped and Ce-doped ZnO thin films.

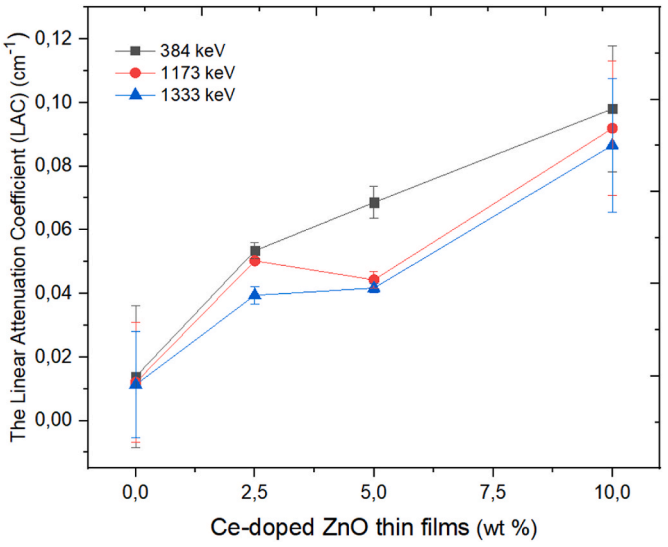

Fig. 8. The Linear Attenuation Coefficient (LAC) of Ce-doped ZnO thin films.

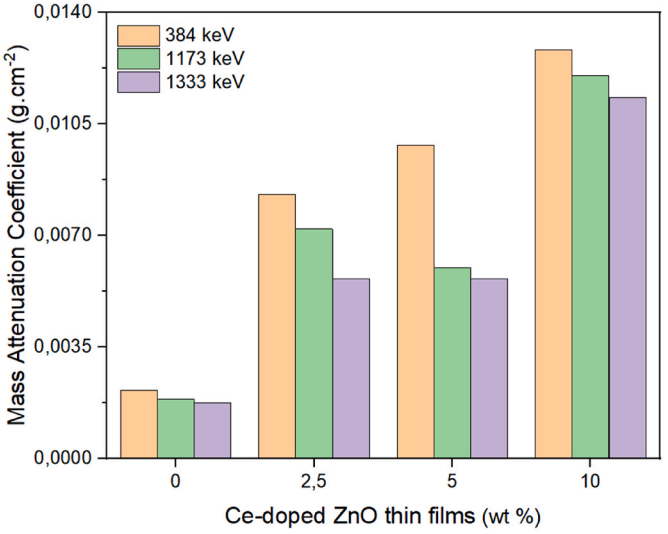

Fig. 9. The Mass Attenuation Coefficient (MAC) of Ce-doped ZnO thin films.

ZnO thin films. Accordingly, while LAC was 0.0138 ± 0.0223 cm^{-1} in undoped films (0 % Ce) at 384 keV, it was 0.0980 ± 0.0198 cm^{-1} at 10 % Ce doping. For gammas with an energy of 1173 keV, this ratio changed between 0.0120 ± 0.0188 cm^{-1} to 0.0919 ± 0.0212 cm^{-1}. Finally, at 1333 keV, the LAC amount decreased from 0.0113 ± 0.0167 cm^{-1} to 0.0865 ± 0.0209 cm^{-1} for the same ratios. As can be seen from these results, the obtained LAC values decrease as the energy increases. Accordingly, it was found that Ce-doped ZnO thin films showed better linear attenuation results at low energies.

The Mass Attenuation Coefficient (MAC) of Ce-doped ZnO thin films can be seen in Fig. 9. Accordingly, while the MAC was 0.0021 ± 0.0031 $cm^2\ g^{-1}$ in Ce-undoped films at 384 keV, it was 0.0128 ± 0.0023 $cm^2\ g^{-1}$ in 10 % Ce-doped films. Other energy values also have a similar trend as in the gamma energy of 384 keV. In the MAC values obtained by dividing the LAC results by the film density, a visible improvement occurred in the MAC results as the energy value increased. In addition, the increase in the Ce ratio in glass positively affected the MAC values.

The Half Value Layer (HVL) of Ce-doped ZnO thin films have been given in Fig. 10. Accordingly, the HVL value at 384 keV gamma energy decreases from 49.97 cm to 7.07 cm as the Ce ratio (0 %–10 % Ce-doped ZnO) increases. HVL values, which is the film thickness required to transmit half of the gammas interacting with the thin film, were positively affected by the energy increase and the required film thickness increased. As can be understood from here, Ce-doped ZnO films do not give positive HVL values at high energies.

The Tenth Value Layer (TVL) of Ce-doped ZnO thin films have been shown in Fig. 11. Accordingly, the TVL value at 384 keV gamma energy decreases from 165.99 cm to 23.49 cm as the Ce ratio (0 %–10 % Ce-doped ZnO) increases. Also, other energies have similar trends. TVL values, which are the film thickness required to transmit one tenth of the gammas interacting with the thin film, were positively affected by the increase in energy, like HVL values, and the required film thickness increased. The increase in the Ce ratio in the glass has made the films more effective in shielding.

Fig. 12 shows the Mean Free Path (MFP) of Ce-doped ZnO thin films. Accordingly, the MFP value at 384 keV gamma energy decreases from 72.09 cm to 10.20 cm as the Ce ratio (0 %–10 % Ce-doped ZnO) increases. According to these results, as the energy of the gammas increases, the distance they can travel through the film increases. The all obtained radiation shielding results have been given in Table 1.

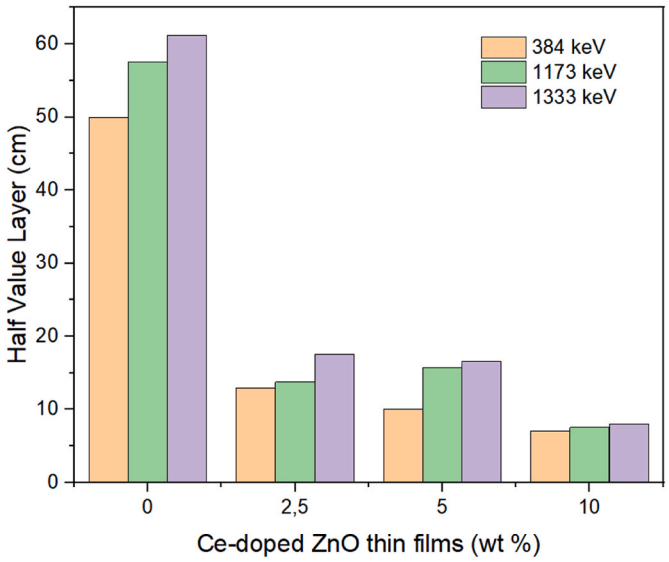

Fig. 10. The Half Value Layer (HVL) of Ce-doped ZnO thin films.

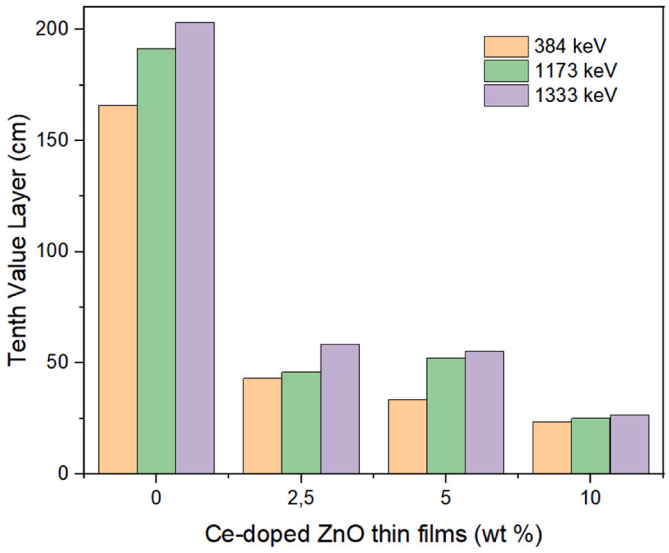

Fig. 11. The Tenth Value Layer (TVL) of Ce-doped ZnO thin films.

4. Conclusion

In this study, pure and Ce-doped ZnO thin films were synthesized by depositing on glass substrate by spray pyrolysis technique. The obtained important results have been given at below:

- XRD analysis showed that ZnO has a wurtzite (hexagonal) structure and CeO_2 has a cubic structure in the synthesized films. It also shows that the (002) diffraction peak is grown along the c-axis of undoped and Ce-doped ZnO thin films. Thus meaning that the incorporation of Ce into ZnO does not cause any effect on the crystal structure of ZnO at the (002) diffraction peak. It was observed that (002) ZnO peak intensity decreased due to cerium additive.
- The average thickness of the synthesized films was measured to be approximately 1.2 μm in SEM images. It was determined that the cerium additive had a positive effect on the surface morphology of the thin film samples.
- It was observed that Ce doping increased the band gap of ZnO from approximately 3.24 to 3.27 (eV).

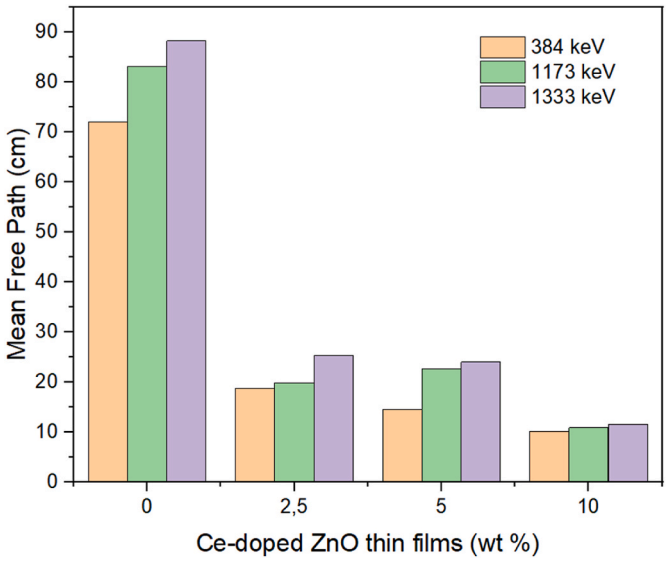

Fig. 12. The Mean Free Path (MFP) of Ce-doped ZnO thin films.

Table 1
Radiation shielding properties of Ce-doped ZnO thin films.

384 keV	μ (cm-1)	ρ (g. cm^{-3})	HVL (cm)	TVL (cm)	MFP (cm)	MAC (cm^2. g^{-1})
0	0.0138 ± 0.0223	6.45	49.9700	165.9967	72.0914	0.0021 ± 0.0031
2.5	0.0534 ± 0.0225	6.98	12.9696	43.0842	18.7112	0.0082 ± 0.00005
5	0.0686 ± 0.0051	7.38	10.1000	33.5514	14.5712	0.0098 ± 0.0008
10	0.0980 ± 0.0198	7.64	7.0716	23.4915	10.2022	0.0128 ± 0.0023
1173 keV						
0	0.0120 ± 0.0188	6.45	57.5998	191.3425	83.0990	0.0018 ± 0.0025
2.5	0.0502 ± 0.0003	6.98	13.7868	45.7986	19.8901	0.0072 ± 0.0002
5	0.0442 ± 0.0027	7.38	15.6568	52.0108	22.5880	0.0059 ± 0.0004
10	0.0919 ± 0.0212	7.64	7.5392	25.0448	10.8768	0.0120 ± 0.0026
1333 keV						
0	0.0113 ± 0.0167	6.45	61.1696	203.2010	88.2491	0.0017 ± 0.0022
2.5	0.0394 ± 0.0027	6.98	17.5769	58.3892	25.3581	0.0056 ± 0.0002
5	0.0416 ± 0.0015	7.38	16.6242	55.2245	23.9837	0.0056 ± 0.0002
10	0.0865 ± 0.0209	7.64	8.0065	26.5970	11.5509	0.0113 ± 0.0026

- It was determined that cerium additive increased optical transmittance. Optical transmittance values are ZnO (78 %), ZnO:Ce2.5 % (85 %), ZnO:Ce5% (87 %), ZnO:Ce10 % (89 %) respectively.
- Radiation shielding properties of Ce-doped ZnO thin films were examined at 384, 1173 and 1333 keV gamma energies.
- MAC values increased from 0.0021 ± 0.0031 cm^2 g^{-1} with 0 % Ce dope to 0.0128 ± 0.0023 cm^2 g^{-1} with 10 % Ce-doped ZnO. HVL, TVL and MFP values were calculated according to the obtained LAC values.
- According to all the results obtained, Ce-doped ZnO thin films show effective results for radiation shielding.

CRediT authorship contribution statement

Ali Kemal Soğuksu: Writing – review & editing, Writing – original draft, Visualization. **Süleyman Kerli:** Writing – review & editing. **Yusuf Kavun:** Writing – review & editing, Visualization. **Ümit Alver:** Writing – review & editing.

Declaration of competing interest

The authors declare that they have no known competing financial interests or personal relationships that could have appeared to influence the work reported in this paper.

Data availability

Data are available from the authors.

Acknowledgment

This study was supported by the Scientific Research Projects Coordination Unit of Kahramanmaraş Sütçü İmam University. Project numbers 2023/6-22 A.

References

[1] A.M. Zeyad, I.Y. Hakeem, M. Amin, B.A. Tayeh, I.S. Agwa, Effect of aggregate and fibre types on ultra-high-performance concrete designed for radiation shielding, J. Build. Eng. 58 (Oct. 2022) 104960, https://doi.org/10.1016/J.JOBE.2022.104960.

[2] R.S.M. Rashid, et al., Effect of elevated temperature to radiation shielding of ultra-high performance concrete with silica sand or magnetite, Construct. Build. Mater. 262 (Nov. 2020) 120567, https://doi.org/10.1016/J.CONBUILDMAT.2020.120567.

[3] I.M. Nikbin, et al., Effect of high temperature on the radiation shielding properties of cementitious composites containing nano- Bi2O3, J. Mater. Res. Technol. 9 (5) (Sep. 2020) 11135–11153, https://doi.org/10.1016/J.JMRT.2020.08.018.

[4] E. Kavaz, N. Ekinci, H.O. Tekin, M.I. Sayyed, B. Aygün, U. Perişanoğlu, Estimation of gamma radiation shielding qualification of newly developed glasses by using WinXCOM and MCNPX code, Prog. Nucl. Energy 115 (Aug. 2019) 12–20, https://doi.org/10.1016/J.PNUCENE.2019.03.029.

[5] H. Eskalen, Y. Kavun, S. Kerli, S. Eken, An investigation of radiation shielding properties of boron doped ZnO thin films, Opt. Mater. 105 (Jul. 2020) 109871, https://doi.org/10.1016/J.OPTMAT.2020.109871.

[6] B. Albarzan, A. Almuqrin, M. K.-P. in N, Effect of Fe2O3 Doping on Structural, FTIR and Radiation Shielding Characteristics of Aluminium-Lead-Borate Glasses, Elsevier, 2021.

[7] A. El-Taher, et al., Gamma ray shielding and structural properties of iron alkali alumino-phosphate glasses modified by PbO, Radiat. Phys. Chem. 165 (2019) 108403, https://doi.org/10.1016/j.radphyschem.2019.108403.

[8] S.A. Issa, H.M.H. Zakaly, M. Pyshkina, M.Y.A. Mostafa, M. Rashad, T.S. Soliman, Structure, optical, and radiation shielding properties of PVA–BaTiO3 nanocomposite films: an experimental investigation, Radiat. Phys. Chem. 180 (Mar. 2021) 109281, https://doi.org/10.1016/J.RADPHYSCHEM.2020.109281.

[9] H. Eskalen, Y. Kavun, S. Kerli, S. E.-O. Materials, and, An Investigation of Radiation Shielding Properties of Boron Doped ZnO Thin Films, Elsevier, 2020.

[10] M. Elsafi, M.A. El-Nahal, M.I. Sayyed, I.H. Saleh, M.I. Abbas, Effect of bulk and nanoparticle Bi2O3 on attenuation capability of radiation shielding glass, Ceram. Int. 47 (14) (Jul. 2021) 19651–19658, https://doi.org/10.1016/J.CERAMINT.2021.03.302.

[11] N. Tamam, et al., Significant influence of Cu content on the radiation shielding properties of Ge-Se-Te bulk glasses, Radiat. Phys. Chem. 193 (Apr. 2022) 109981, https://doi.org/10.1016/J.RADPHYSCHEM.2022.109981.

[12] J. Singh, V. Kumar, Y.K. Vermani, M.S. Al-Buriahi, J.S. Alzahrani, T. Singh, Fabrication and characterization of barium based bioactive glasses in terms of physical, structural, mechanical and radiation shielding properties, Ceram. Int. 47 (15) (Aug. 2021) 21730–21743, https://doi.org/10.1016/J.CERAMINT.2021.04.188.

[13] G. Kilic, E. Ilik, S.A. M Issa, B. Issa, M.S. Al-Buriahi, U.G. Issever, H.O. Tekin, Ytterbium (III) oxide reinforced novel TeO2–B2O3–V2O5 glass system: synthesis and optical, structural, physical and thermal properties, Ceram. Int. 47 (13) (2021) 18517–18531, https://doi.org/10.1016/j.ceramint.2021.03.17.

[14] M. Rashad, H.A. Saudi, Hesham M.H. Zakaly, Shams A.M. Issa, Alaa M. Abd-Elnaiem, Control optical characterizations of Ta+5–doped B2O3–Si2O–CaO–BaO glasses by irradiation dose, Opt. Mater. 112 (2021) 110613.

[15] H.A. Saudi, Hesham M.H. Zakaly, Shams A.M. Issa, H.O. Tekin, M.M. Hessien, Y. S. Rammah, A.M.A. Henaish, Fabrication, FTIR, physical characteristics and photon shielding efficacy of CeO_2/sand reinforced borate glasses: experimental and simulation studies, Radiat. Phys. Chem. 191 (February 2022) 109837.

[16] J.V. Soni Gyanesh, Gouttam Niharika, "Synthesis and comparisons of Optical and Gamma Radiation shielding properties for ZnO and SiO2 nanoparticles in PMMA nanocomposites thin films,", Optik 259 (2022) https://doi.org/10.1016/j.ijleo.2022.168884.

[17] O.M.S. Rajendran, R. Kannan, An electrochemical investigation on PMMA/PVdF blend-based polymer electrolytes, Mater. Lett. (2001), https://doi.org/10.1016/S0167-577X(00)00363-3.

[18] G. Soni, S. Srivastava, P. Soni, P. Kalotra, Y.K. Vijay, Optical, mechanical and structural properties of PMMA/SiO2 nanocomposite thin films, Mater. Res. Express 5 (1) (Jan. 2018), https://doi.org/10.1088/2053-1591/AAA0F7.

[19] G. Soni, P. Soni, P. Jangra, Y.K. Vijay, Optical, mechanical and thermal properties of PMMA/graphite nanocomposite thin films, Mater. Res. Express 6 (7) (Apr. 2019) 075315, https://doi.org/10.1088/2053-1591/AB1327.

[20] L. Chuah, H. Abdulgafour, Z.H.-T. Ijes, "Preparation of Aluminum Foil-Supported ZnO Nanocoral Reef Films," theijes.comLS Chuah, HI Abdulgafour, Z HassanThe IJES, 2013•theijes.com, 2013, pp. 2–4.

[21] K. Davis, R. Yarbrough, M. Froeschle, J. W.-R, "Band Gap Engineered Zinc Oxide Nanostructures via a Sol–Gel Synthesis of Solvent Driven Shape-Controlled Crystal Growth," pubs.rsc.Org, 2019. K Davis, R Yarbrough, M Froeschle, J White, H RathnayakeRSC Adv. 2019•pubs.rsc.org.

[22] M. Bouderbala, S. Hamzaoui, B.A.-P. B. C, Thickness Dependence of Structural, Electrical and Optical Behaviour of Undoped ZnO Thin Films, Elsevier, 2008.

[23] M. Faraj, K. I.-I. J. of P. Science, "Optical and Structural Properties of Thermally Evaporated Zinc Oxide Thin Films on Polyethylene Terephthalate Substrates," hindawi.comMG Faraj, K IbrahimInternational J. Polym. Sci. 2011•hindawi.Com, 2011.

[24] S. Bharath, K. Bangera, S.-S. G, Enhanced Gas Sensing Properties of Indium Doped ZnO Thin Films, Elsevier, 2018.

[25] M. Koç, Ultrasonik Sprey Piroliz ile Üretilen ZnO İnce Filmlerin Alttaş Sıcaklıklarının Yapısal ve Optik Özelliklerine Etkisi, Süleyman Demirel Üniversitesi Fen Edeb. Fakültesi Fen Derg. 16 (1) (May 2021) 169–178, https://doi.org/10.29233/SDUFEFFD.911477.

[26] M. Socol, N. Preda, A. Costas, A.S. C. B, Hybrid Organic-Inorganic Thin Films Based on Zinc Phthalocyanine and Zinc Oxide Deposited by MAPLE, Elsevier, 2020.

[27] S.K.-O. Materials, Al Doped ZnO Thin Films Obtained by Spray Pyrolysis Technique: Influence of Different Annealing Time, Elsevier, 2021.

[28] Z. Yan et al., "Impacts of Preparation Conditions on Photoelectric Properties of the ZnO: Ge Transparent Conductive Thin Films Fabricated by Pulsed Laser Deposition," Elsevier.

[29] Y. Xiang et al., "Physical Properties Revealed by Transport Measurements for Superconducting Nd0. 8Sr0. 2NiO2 Thin Films," *iopscience.iop.Org*, Y Xiang, Q Li, Y Li, H Yang, Y Nie, HH WenChinese Phys. Lett. 2021•iopscience.iop.org..

[30] R. Ghane-Motlagh, P. W.-S. M. and Structures, "A Pyroelectric Thin Film of Oriented Triglycine Sulfate Nano-Crystals for Thermal Energy Harvesting," iopscience.iop.orgR Ghane-Motlagh, P WoiasSmart Mater. Struct. 2019•iopscience.iop.Org, 2019.

[31] M. Laurenti, N. Garino, N. Garino, G. Canavese, S. Hernandéz, V. Cauda, Piezo- and photocatalytic activity of ferroelectric ZnO:Sb thin films for the efficient degradation of rhodamine-β dye pollutant, ACS Appl. Mater. Interfaces 12 (23) (Jun. 2020) 25798–25808, https://doi.org/10.1021/ACSAMI.0C03787.

[32] R.D.-M. Symposia, Influence of spray solution quantity on microstructural and optical properties of In2O3 thin films prepared by spray pyrolysis, in: DeokateMacromolecular Symp. 2020•Wiley Online Libr, 392, Wiley Online Libr, 2020, https://doi.org/10.1002/masy.201900152, 1, Aug. 2020.

[33] A. Sudha, T. Maity, S. Sharma, M.S. A. G, An Extensive Study on the Structural Evolution and Gamma Radiation Stability of TeO2 Thin Films, Elsevier, 2018.

[34] M. Yousefi, M. Amiri, R. Azimirad, A.M.-J. of Electroanalytical, Enhanced Photoelectrochemical Activity of Ce Doped ZnO Nanocomposite Thin Films under Visible Light, Elsevier, 2011.

[35] H. Zhang, Z.J. Optik, Application of Porous Silicon Microcavity to Enhance Photoluminescence of ZnO/PS Nanocomposites in UV Light Emission, Elsevier, 2017.

[36] S. Tijani, S. Kamal, Y. Al-Hadeethi, M.A. J. of A, Radiation Shielding Properties of Transparent Erbium Zinc Tellurite Glass System Determined at Medical Diagnostic Energies, Elsevier, 2018.

[37] M. Duinong, et al., Effect of gamma radiation on structural and optical properties of ZnO and Mg-doped ZnO films paired with Monte Carlo simulation, mdpi.comM Duinong, R Rasm. FP Chee, PY Moh, S Salleh, KA Mohd Salleh, S IbrahimCoatings, 2022•mdpi.com (2022), https://doi.org/10.3390/coatings12101590.

[38] H.A. Thabit, N.A. Kabir, A. Khamim Ismail, S. Alraddadi, A. Bafaqeer, M.A. Saleh, Development of Ag-Doped ZnO Thin Films and Thermoluminescence (TLD) Characteristics for Radiation Technology, mdpi.com, 2022, https://doi.org/10.3390/nano12173068. HA Thabit, NA Kabir, AK Ismail, S Alraddadi, A Bafaqeer, MA SalehNanomaterials, 2022•mdpi.com.

[39] W. Zhang et al., "Structural, Optical and Electrical Properties of Sol-Gel Spin-Coated Ga and F Co-doped ZnO Films,"Elsevier..

[40] Y. Kavun, S. Kerli, H. Eskalen, M. K.-R. P. and Chemistry, Characterization and Nuclear Shielding Performance of Sm Doped In_2O_3 Thin Films, Elsevier, 2022.

[41] H. Eskalen, Y. Kavun, M. K.-A. R. and Isotopes, Preparation and Study of Radiation Shielding Features of ZnO Nanoparticle Reinforced Borate Glasses, Elsevier, 2023.

[42] Y. Kavun, H. Eskalen, M. K.-C. P. Letters, A Study on Gamma Radiation Shielding Performance and Characterization of Graphitic Carbon Nitride, Elsevier, 2023.

[43] C.K. Kasar, U.S. Sonawane, J.P. Bange, D.S. Patil, Optical and structural properties of nanoscale undoped and cerium doped ZnO with granular morphology, J. Mater. Sci. Mater. Electron. 27 (11) (Nov. 2016) 11885–11889, https://doi.org/10.1007/S10854-016-5333-4.

[44] N.F. Djaja, R. Saleh, Characteristics and photocatalytics activities of Ce-doped ZnO nanoparticles, Materials Sciences and Applications 4 (02) (2013) 145.
[45] M. Sowjanya, M. Shariq, S. Pilli, . M. K.-E, "Impact of Ar: O2 Gas Flow Ratios on Microstructure and Optical Characteristics of CeO2-Doped ZnO Thin Films by Magnetron Sputtering," iopscience.iop.Org, 2021.
[46] M. Salem, S. Akir, I. Massoudi, Y. Litaiem, M. Gaidi, K. Khirouni, Enhanced photoelectrochemical and optical performance of ZnO films tuned by Cr doping, Appl. Phys. Mater. Sci. Process 123 (4) (Apr. 2017), https://doi.org/10.1007/S00339-017-0880-Y.
[47] A. Bera, S. Chattopadhyay, Optical properties of Fe-doped ZnO thin film on p-Si by spin coating, Lect. Notes Electr. Eng. 575 (2020) 387–395, https://doi.org/10.1007/978-981-13-8687-9_35.
[48] Q. Luo, et al., Blue luminescence from Ce-doped ZnO thin films prepared by magnetron sputtering, Appl. Phys. Mater. Sci. Process 108 (1) (Jul. 2012) 239–245, https://doi.org/10.1007/S00339-012-6883-9.